Citation for published version:
Gris-Sanchez, I & Knight, JC 2012, 'Time-dependent degradation of photonic crystal fiber attenuation around OH absorption wavelengths', Journal of Lightwave Technology, vol. 30, no. 23, pp. 3597-3602. https://doi.org/10.1109/JLT.2012.2223453

DOI:
10.1109/JLT.2012.2223453

Publication date:
2012

Document Version
Peer reviewed version

Time-dependent degradation of photonic crystal fiber attenuation around OH^- absorption wavelengths

I. Gris-Sanchez and J. C. Knight

***Abstract*—We present a study of the time-dependent degradation of attenuation in Photonic Crystal Fibers in the wavelength region from 1350 to 1450nm. Changes in spectral attenuation were monitored over 16 weeks of exposure to a laboratory environment in different solid core PCF's as well as in a hollow-core bandgap fiber. Increasing spectral attenuation was observed at 1364nm and at 1384nm, wavelengths corresponding to known OH^- absorption features. We also observe the appearance of a broad attenuation peak around 1398nm. The observed degradation is shown to decrease exponentially from the ends of the fiber, and is attributed to ingress of contaminants from the fiber ends. This attribution is supported by measurements on a fiber stored with sealed ends.**

***Index Terms*—aging, low loss Photonic Crystal Fiber, degradation, OH contamination**

I. Introduction

THE holes running along the length of a solid-core Photonic Crystal Fiber (SC-PCF) or of a hollow core band-gap photonic crystal fiber (HC-PCF) make these fibers potentially prone to contamination and consequently to degradation of their optical performance. The presence of air holes – to form either a hollow core or a photonic crystal cladding, or both, is fundamental to the performance of the fibers, conferring multiple benefits on fiber performance [1][2]. Nonetheless it may prove a handicap for the many applications where low spectral attenuation is a requirement, for example in soliton self-frequency shift experiments [3] or CW supercontinuum generation [4]. In addition mechanical failure in standard optical fibers is associated with corrosion also caused by OH^- diffusion and formation (following hydrogen diffusion) in the silica glass [5]. In the present work we performed a series of experiments with 3 low loss SC-PCF's (Fig. 1) and a HC-PCF (Fig. 2) fabricated for these measurements. In the first experiment the fibers were left exposed to laboratory conditions and the transmission through the fiber length was monitored over 16 weeks in the wavelength range from 1350 nm to 1450 nm. In the second experiment, performed at the end of this period, we gradually cut the fibers back from the ends in order to locate the degraded length. In a third parallel set of measurements, we performed initial transmission measurements through an identical set of fibers before fusing their ends. After two months the fiber seals were broken and a second measurement was taken on these fibers.

Manuscript received May 17, 2012. (Write the date on which you submitted your paper for review.) I.Gris-Sanchez wants to thank the National Council of Science and Technology CONACyT (Mexico) for financial support.

I. Gris-Sanchez Author is with University of Bath, BA2 7LY, Bath, United Kingdom (corresponding author phone: +44(0)1225-583-; e-mail: I.Gris.Sanchez@bath.ac.uk).

J. C. Knight Author, is with University of Bath, BA2 7LY, Bath, United Kingdom (e-mail: j.c.knight@bath.ac.uk).

II. Experiments

The PCF's used in the experiments were specially fabricated with low OH^- absorption by annealing the preform prior to fiber draw [6]. The spectral attenuation and scanning electron microscope images of the PCF's are shown in Fig. 1 and Fig. 2. The core diameter and cladding hole diameters are shown in table 1. The low-loss transmission window of the HC-PCF (fiber D) was centered at 1365 nm.

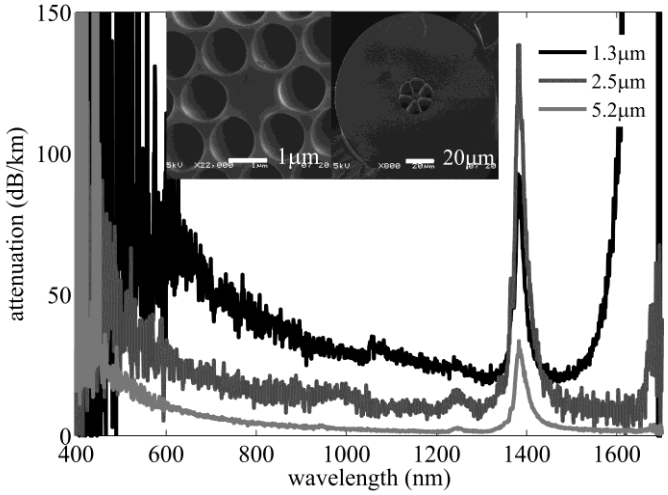

Fig. 1. Spectral attenuation of the solid-core PCF's used to monitor degradation. Core diameters: fiber A 1.3 μm, fiber B 2.5 μm and fiber C 5.2 μm. Inset: SEM pictures left fiber A, right fiber C.

TABLE I

DRAW PARAMETERS

fiber	Type	Φ_{clad} (µm)	Φ_{core} (µm)	DDR
A	SC-PCF	1.16	1.3	15384
B	SC-PCF	1.8	2.26	8810
C	SC-PCF	9.44	5.2	3846
D	HC-PCF	3.4	10.3	N/A

Φ_{clad}: cladding holes (surrounding the core) diameter

Φ_{core}: fiber core diameter

DDR: total draw down ratio (core)

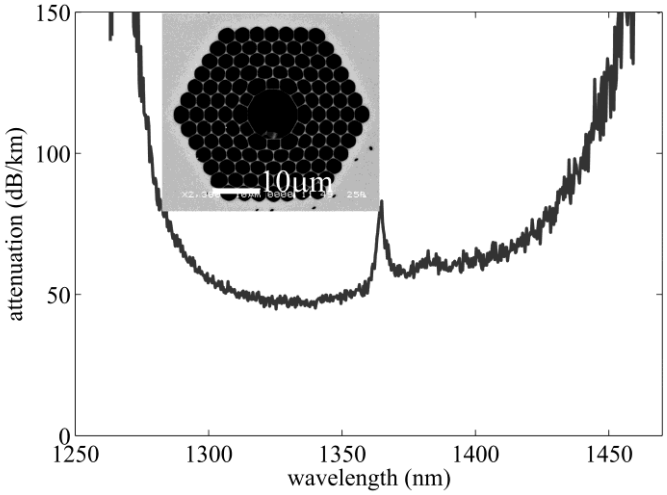

Fig. 2. Spectral attenuation of the HC-BG-PCF (fiber D) with the band gap centered around 1365 nm used to monitor degradation.

A. Time dependence of PCF transmission

To study the effects of atmospheric exposure on fiber attenuation, three SC-PCF's and one HC-PCF were left with unprotected ends exposed to uncontrolled laboratory conditions. Relative humidity (R. H. %) varied from 30% to 50 %, and temperature from 22°C to 25°C. All the fibers were wound around spools of 10 cm in radius; no bending losses were observed at to this radius of curvature. Spectral transmission of the fibers was measured regularly in the range 1350 nm to 1450 nm over a 16 week period. As an example Fig. 3 shows transmission measurements recorded over time for fiber A.

The experiment consisted of coupling white light (an optical fiber-based supercontinuum source) into the core of the fiber under test and then recording the transmitted spectrum using an optical spectrum analyzer (OSA). The lengths used for the measurements were 25 m for fibers A and B, 35 m for fiber C and 50 m for fiber D. The different lengths were chosen to allow us to track the changes in each fiber's transmission even after high levels of degradation and yet to observe the OH absorption peaks in the first measurement. Peaks at 1364 nm, attributed to surface OH^- [7], and at 1384 nm (well-known as the first OH^- stretching overtone) were spectrally resolved. In Fig. 4, the increase in absorption is presented for all fibers at 1384 nm. The data points for fibers A and C were in each case collected from two identical fibers for practical reasons, giving a break in the curves but no real change in the trend. The absorption strength at 1364 nm was also increasing (not shown) but was not as strong as that at 1384 nm, whereas the absorption at 1398 nm (not shown) was stronger than at 1384 nm after a few weeks.

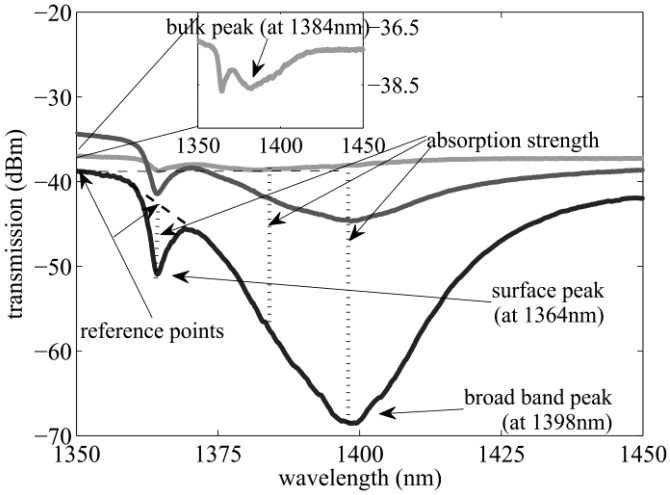

Fig. 3. Transmission for fiber A (1.3 µm) for different exposure times. From light gray to dark gray the exposure time was: day 0, week, 4 and week 22 (the different signal level is due to a difference in the input coupling). Dotted lines illustrate the absorption strength (modulus of the difference between the reference points and the wavelengths 1364 nm, 1384 nm and 1398 nm). The inset is a *y*-axis zoom of the first measurement.

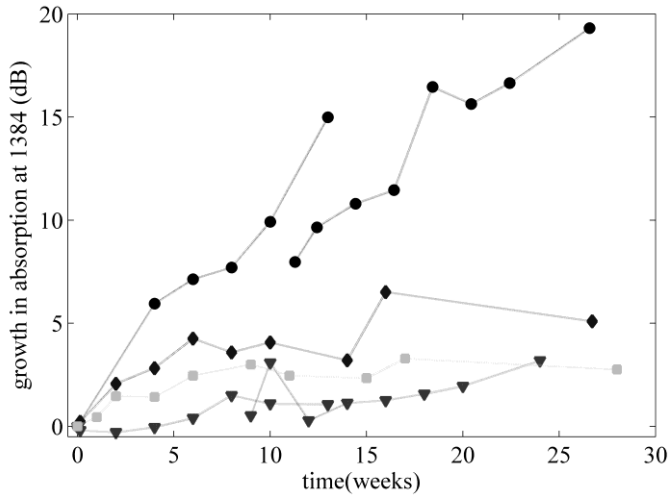

Fig. 4. Growth of the absorption at 1384 nm for different core sizes 1.3 µm (circles), 2.5 µm (rhombus), 5.2 µm (triangles), and HC-PCF (squares).

B. Localization of degradation

At the end of the time evolution experiment the same fibers were used to identify the length dependence of the increased attenuation at the contaminated ends. White light was coupled into one end of the fiber. We repeatedly cut off a short length of fiber at the output end, and measured the transmission through the remainder each time. Fig. 5 illustrates the transmission spectra for this experiment using fiber B. In Fig. 6 we present the normalized transmission for the peaks at 1364 nm, 1384 nm and 1398 nm in relation to the lengths removed.

When the spectral features being studied showed no further change we turned the fiber around, coupling light into the former output end and measuring the output whilst we continued to cut the fiber from the other end until the spectrum again did not change. The diamonds and exponential fits on the left hand side of Fig. 6 denote the measurements for cutting back lengths from the first end (0, 0.1, 0.2, 0.5, 1, 1.5, 2, 2.5 and 3 m). The diamonds and fits on the right hand side show the continued measurements for the other end according to their fiber position (25, 24.9, 24.8, 24.5, 24, 23.5, 23, 22.5, 22, and 21.5 m) once the ends had been exchanged.

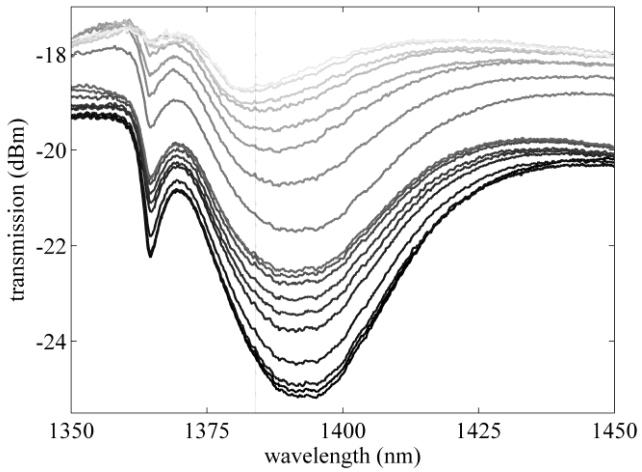

Fig. 5. Cut back transmission measurements of the 2.5 µm core fiber for different lengths. Starting from 25 m (bottom) to 21.5 m on one end, and from 21.5 m to 18 m (top).

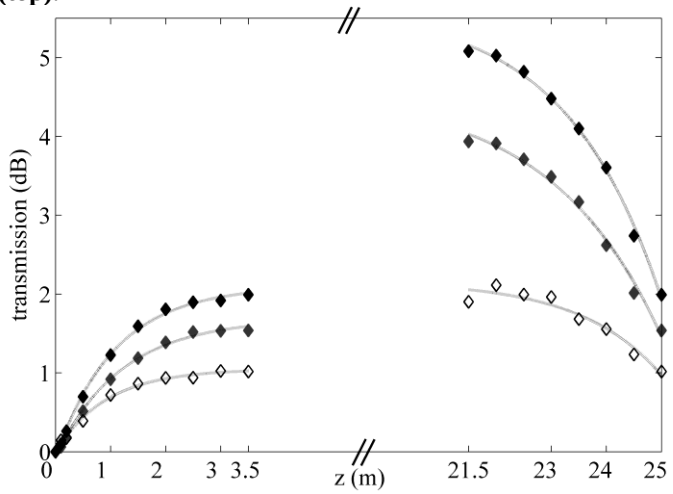

Fig. 6. Transmission of different absorption bands for fiber B (2.5 µm core diameter). The dotted lines correspond to the exponential fits and diamonds to data points at 1364 nm (white), 1384 nm (gray) and 1398 nm (black), z is the fiber length. The transmission increases as the contaminated ends are chopped. On the left the comparison for fiber B at one fiber end.

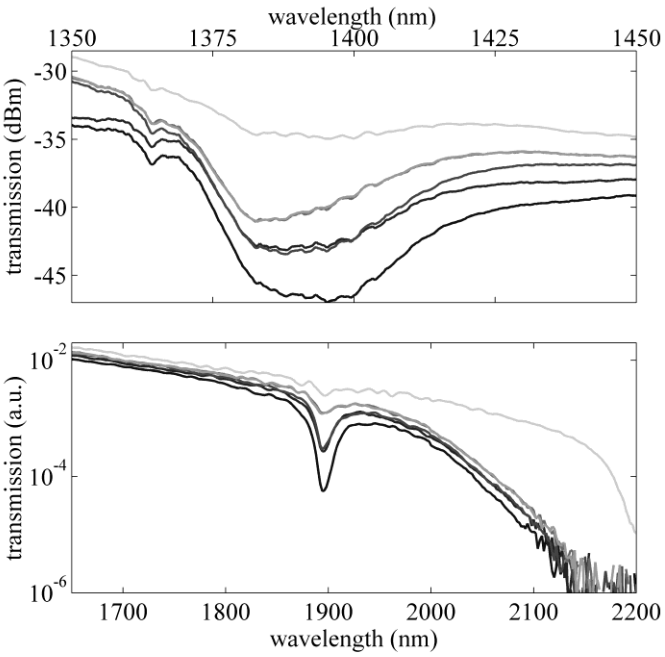

Fig. 7. Transmission (from 1350 nm to 1450 nm and from 1650 nm 2200 nm) for a low loss 5µm core fiber exposed over 2 years to atmospheric conditions. Transmission measured over (in both wavelengths ranges from bottom to top) 249 m, 243 m and recoupling onto the other end 243 m, 237 m and 50 m.

When exploring the transmission spectra for longer wavelengths through a different fiber (similar in design to fiber C with a core diameter of 5µm) an absorption peak was detected around 1900 nm. This fiber had been left open to laboratory conditions for a period of 2 years. For the measurements a supercontinuum was used as light source. The fiber length was 249 m. The transmitted spectrum was recorded using an OSA from 1350 nm to 1450nm and from 1600 nm to 2200 nm with a Bentham spectrometer. The spectra was measured over 249 m, 243 m (6 m chopped from the first end), 237 m (6 m more cut off from the second end), and finally over 50 m.

Fig. 7 shows the transmission for the different fiber lengths.

C. Fiber with sealed ends

Identical lengths of the fibers A, C and D were sealed shortly after fabrication, after measuring the transmission, by fusing both ends with a fiber splicer. After 11 weeks the seals were broken by carefully cleaving off the fused ends. The transmission was measured again under the same conditions as before. In table II we present the absorption at 1364 nm and 1384 nm before and after end sealing.

TABLE II
ABSORPTION MEASURED BEFORE END SEALING AND AFTER 11 WEEKS AND 2 DAYS FOR FIBERS A, C AND D AT 1364 AND 1384 NANOMETERS.

fiber	Absorption at1364 nm (dB)		Absorption at1384 nm (dB)	
	Before end sealing	After 11 weeks	Before end sealing	After 11 weeks
A	1.24	1.37	1.57	1.25
C	0.02	0.43	1.10	1.71
D	1.68	1.64	1.35	2.29

III. DATA ANALYSIS

Although a tungsten lamp was used as a source to obtain the attenuation measurements shown in Fig. 1, in order to obtain high-resolution measurements of the changes in the transmission with time we used an optical supercontinuum. The source spectrum was recorded (not shown) for each measurement.

The method used to calculate the strength of the OH^- related absorption peak is described below:

1. The raw transmission data sets obtained from each fiber were divided by the corresponding supercontinuum spectra in order to get rid of the spectral contribution of the supercontinuum, then the corrected spectra (shown in Fig. 3), were used to calculate the strength of the absorption related to OH^- bands.
2. Absorption was calculated relative to a reference point at a nearby wavelength. For absorption at wavelengths 1384 nm and 1398 nm we used the transmission at 1350 nm as a reference point (see Fig. 3). For the absorption strength of the surface peak at 1364 nm we calculated a straight line joining the transmission at 1360nm and 1370nm, and used the value of that line at 1364 nm as reference (see Fig. 3).

In Fig. 4 the values of the absorption strength for each fiber are referenced to the value of the initial measurements.

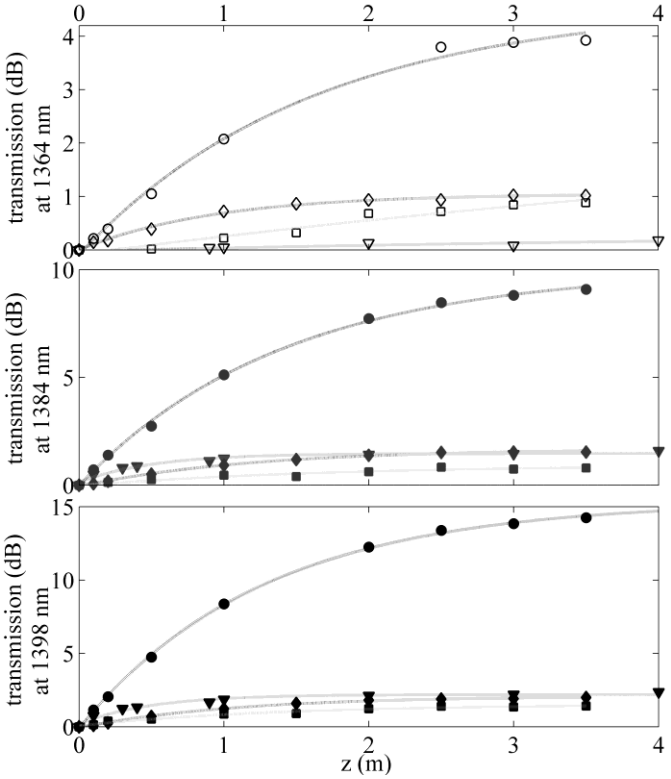

Fig. 8. Comparison of the exponential fits and experimental normalized transmission for the localization of degradation at one of the contaminated ends. From top to bottom 1364 nm, 1384 nm and 1398 nm. Data points: circles correspond to a diameter of 1.3 μm , diamonds to 2.5 μm, triangles to 5.2 μm and squares correspond to the HC-PCF.

To model the position dependent local attenuation (of the contaminated fiber ends) we make the assumption that the attenuation due to contamination is high compared to the original attenuation and that the contaminated length is short compared to the total fiber length. The data obtained (cutback transmission measurements) from the localization of degradation experiment (shown in Fig. 8 for fiber B) were fitted to the exponential model described in eq. 1

$$y(x) = ae^{bx} + c \tag{1}$$

y is the logarithm of the transmission (in dB) that depends exponentially on distance x (in m), where a (in dB) is a scaling factor and $a+c$ (in dB) is the initial value at $y(0)$, $b>0$ (in m^{-1}) is the growth rate per unit length and c is absorption (assumed constant) in the uncontaminated fiber. The positive sign is used in the exponential to reflect that fact that our measurements are done by cutting back from the end of the fiber. The local attenuation α (Fig. 9) at every point of the contaminated end was obtained by taking the derivative of the (exponential) fit to the experimental transmission measurements (eq. 1) multiplied by a 1000 factor:

$$\alpha(x) = 10^3 a \cdot b\, e^{bx} \tag{2}$$

where α is in dB/km

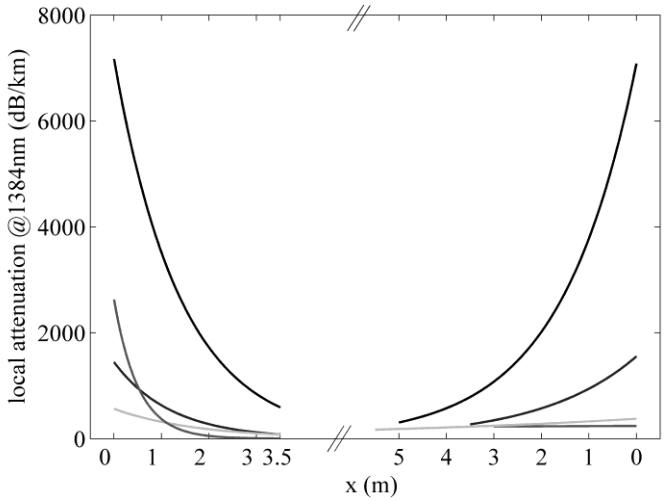

Fig. 9. Local attenuation for all fibers at 1384 nm, x is the length from the end to the center of the fibers. From black to light gray 1.3 μm, 2.5 μm, 5.2 μm core diameter and HC-PCF (fibers A, B, C and D).

IV. RESULTS AND DISCUSSION

The PCF's were fabricated with low attenuation (Fig. 1 and Fig. 2). Indeed, our interest was to establish how such low OH^- content fibers degraded with time (Fig. 3), even after only a few days of exposure, at 1364 nm and 1384 nm. For the time-dependence experiment an increase in the absorption bands is observed in all the SC-PCF's (see Fig. 4)). Fig. 3 illustrates the changes over time in the spectrum of fiber A. Also a broad absorption feature at 1398nm was detected in all the SC-PCF, which became stronger after a few weeks of exposure to the laboratory conditions.

In the spectra obtained for fiber D we observe a fine

structure (Fig. 10, Fig. 11 and Fig. 12) that corresponds to the absorption lines of atmospheric water vapor [8]. High spectral resolution (0.1nm) transmission measurements using a supercontinuum source for fiber D and a tungsten lamp source using a 9 m piece of commercial SMF-28 instead of the fiber under test are also shown in Fig. 11 and Fig. 12. We attribute the lines in the spectrum obtained when using the SMF-28 to the presence of atmospheric OH^- both in the laboratory and within the OSA. The increased strength of these water vapor lines when using the PCF is attributed to the presence of water vapor in the cladding holes of fiber D. Water in contact with the silica surface reacts, creating OH^- ions [9] which subsequently diffuse to the silica core (in the case of a SC-PCF). Note that the HC-PCF under study also presents a broadband feature (Fig. 10) similar to that for SC-PCF's.

The generalized increase in the background absorption (visible in Fig. 5) can be attributed to the increase of scattering on the core surface of the contaminated fiber ends which are covered by OH^- groups. After removing the contaminated ends the overall loss decreases to the original levels including the absorption bands at 1364 nm, 1384 nm and 1398 nm as seen in Fig. 5.

According to Hanafusa et al. [10] and Yin [11] the concentration of defect centers is larger on the surface than within the fiber core. For a cylinder (i.e the fiber core) the surface to volume relation is $2/r$ where r is the core radius, so that for a fixed volume of silica more of that material is on the surface as r gets smaller. Also there is a relationship between the number of defects and the thermal history of the preform (the number of defects increases with increasing fictive temperature (T_f) [12]). The abundance and mobility of OH^- groups in silica is linked to the number of site defects or broken Si-O bonds [12]. The degradation of the different fibers as observed in Fig. 4 is therefore related to the number of defects on the silica surface given by the T_f. Consequently, more defects lead to more OH^- formation and to its subsequent diffusion to the fiber core being more evident for 1.3μm fiber (fiber A).

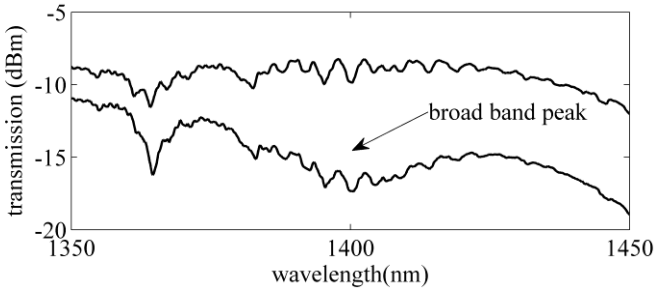

Fig. 10. Fiber D transmission spectrum measured just after fabrication (top), and after 28 weeks of exposure (bottom). Note the surface peak growth and the appearance of a broad absorption feature.

Although the drawing temperature and speed were kept roughly the same for all the SC-PCF's there is a large difference in the draw down ratios (DDR) of the different fibers, in particular between fiber A and C (see Table 1). We have defined the DDR as the scaling factor between the diameter of the original silica rod as purchased and the corresponding core diameter in the final fiber. Note that despite the fact that the cladding holes surrounding the core of fiber C are larger than those for fibers A and B (see Table I) the increase in local attenuation, is not larger for fiber C than that observed for fiber A and B at the fiber ends. This is perhaps due to lower number of structural defects in larger core fibers with smaller DDRs.

For fiber A the absorption grows at a notably faster rate than in fibers B and C. This rapid degradation by OH^- contamination in small core fibers recalls the dramatic increase at 1384nm for small core PCF's (below 2μm) [6] which suggests a similar or related origin.

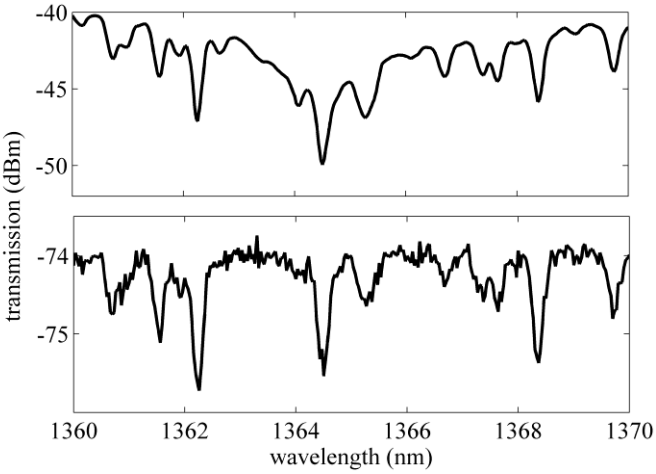

Fig. 11. Comparison of the fine spectral absorption bands of atmospheric water vapor [8] observed in the range from 1360 nm to 1370 nm (top fiber D bottom SMF-28).

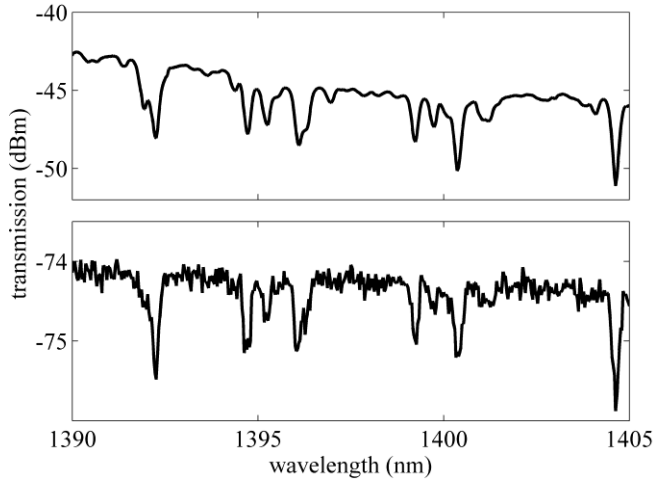

Fig. 12. Comparison of the fine spectral absorption bands of atmospheric water vapor [8] observed in the range from 1390 nm to 1405 nm (top fiber D bottom SMF-28).

In Fig. 6 the localization of degradation (for 1364 nm, 1384 nm, and 1398 nm) to the fiber ends is demonstrated for fiber B along with the exponential fits. In Fig. 8 experimental data and fitted curves are compared for all fibers (all normalized to start at zero dB). The coefficients of the fits obtained for 1364 nm, 1384 nm, and 1398nm are included in Table III. Note that a higher value of b corresponds to the contamination occurring

over a shorter length of fiber. The position dependent local values of attenuation in the contaminated ends (plotted in Fig. 9) were obtained by calculating the derivative of the exponential fits.

TABLE III
b COEFFICIENT FOR FIBER B, C AND D FOR DIFFERENT WAVELENGTHS

fiber	@1364 nm [m^{-1}]	@1384 nm [m^{-1}]	@1398 nm [m^{-1}]
A end 1	0.6218	0.7131	0.7863
A end 2	0.8969	0.6277	0.7599
B end 1	1.075	0.8307	0.9221
B end 2	0.6887	0.4994	0.5785
C end 1	0.1852	1.958	1.98
C end 2	N/A	N/A	N/A
D end 1	0.1124	0.574	0.731
D end 2	0.138	0.1437	0.1631

Finally

Fig. 7 shows the transmission measurements of a different 5 µm core fiber at longer wavelengths where a peak centered at 1900 nm (which has not been reported for SC-PCF's) appears to be related to the surface, bulk and broad peaks. The absorption of the peaks is reduced as the contaminated ends are cut off. Walrafen and Stone [13] reported an absorption band for the combination of the fundamental OH^- stretching mode and the second SiO_4 vibration mode ($\nu_3+2\nu_1$) located at 1894nm but we cannot identify that in our observations.

The absorption at 1364 nm and 1398 nm before and after the end sealing of the fibers A, C and D did not have major changes compared to the unprotected fibers ends

V. CONCLUSION

An increase in absorption is observed in all fibers at 1384 nm, 1398 nm (observable for all the SC-PCF's) and at 1365 nm (present in all fibers) following fiber exposure to atmospheric conditions, with the smallest-core fiber being the most affected. The increased absorption occurs from the cleaved fiber ends and we attribute it to ingress of contaminants from the atmosphere.

Original levels of absorption are recovered after removing the contaminated ends.

End sealing effectively protected the PCF's from OH^- contamination, confirming that atmospheric water vapor enters the fiber through the cladding holes.

We expect that standard PCF's would also degrade with time provided that the core is not saturated with OH. The degradation will vary according to the core size and thermal history, and the solubility of OH might be higher for standard PCF's whose preform has not been annealed [14].

The development of widely tunable sources for bio-medical or telecommunications applications requires low attenuation, and so it would be of interest to understand the cause of the absorption band at 1900 nm. We speculate that the origin of this absorption band is related to the diffusion of contaminants (i.e. OH^-) interacting with the silica network, as the peak absorption intensity was reduced after removing the contaminated ends.

ACKNOWLEDGMENT

I. Gris-Sanchez wants to acknowledge Dr. B. J. Mangan for fabricating fiber D.

REFERENCES

[1] R. F. Cregan, B. J. Mangan, J. C. Knight, T. A. Birks, P. St. J. Russell, P. J. Roberts, and D. C. Allan, "Single-mode photonic band gap guidance of light in air," *Science*, vol. 285 (5433), pp. 1537-1539, 1999.

[2] T. M. Monro, W. Belardi, K. Furusawa, J. C. Baggett, N. G. R. Broderick, and D. J. Richardson, "Sensing with microstructured optical fibers," *Meas. Sci. Tech*. vol. 12(7), pp. 854-858, 2001.

[3] S. Dekker, A. C. Judge, R. Pant, I. Gris-Sánchez, J. C. Knight, C. M. de Sterke, and B. J. Eggleton, "Highly-efficient, octave spanning soliton self-frequency shift using a specialized photonic crystal fiber with low OH loss.," *Optics express* vol. 19(18), pp. 17766-73, 2011.

[4] J. C. Travers, R. E. Kennedy, S. V. Popov, J. R. Taylor, H. Sabert, and B. Mangan, "Extended continuous-wave supercontinuum generation in a low-water-loss holey fiber," *Opt. Lett*. Vol. 30(15), pp. 1938–1940, 2005.

[5] K.H. Chang, J.P. Fletcher, J. Rennell, A. Nakajima, J. Vydra, and R. Sattmann, "Next generation fiber manufacturing for the highest performing conventional single mode fiber," *Optical Fiber Communication Conference*, 2005. Technical Digest. OFC/NFOEC , vol.3, pp. 6-11, 2005.

[6] I. Gris-Sánchez, B.J. Mangan, and J.C. Knight, "Reducing spectral attenuation in small-core photonic crystal fibers," *Opt. Mater. Express* vol. 1(2), pp.179-184, 2011.

[7] R. Bise and D. Trevor, "Surface absorption in microstructured optical fibers," in *Optical Fiber Communication Conference, Technical Digest* (CD) (Optical Society of America, 2004), paper WI4.

[8] J. A. Curcio, L. F. Drummeter, and G. L. Knestrick, "An Atlas of the Absorption Spectrum of the Lower Atmosphere from 5400Å to 8520Å," *Appl. Opt.* vol. 3(12), pp. 1401-1409, 1964.

[9] R. K. Iler, The Chemistry of Silica (John Wiley and Sons, New York, 1979, Chap 6.

[10] H. Hanafusa and Y. Hibino and F. Yamamoto, "Formation mechanism of drawing-induced E' centers in silica optical fibers," *J. Appl. Phys.* vol. 58(3), pp. 1356-1361, 1985.

[11] Z. Yin and Y. Jaluria, "Neck down and thermally induced defects in high-speed optical fiber drawing," *J. heat transfer* vol. 122(2), pp. 351-362, 2000.

[12] R. H. Stolen and G. E. Walrafen, "Water and its relation to broken bond defects in fused silica," *J. Chem Phys.* vol. 64(6), 2623, 1976.

[13] J. Stone and G. E. Walrafen, "Overtone vibrations of OH groups in fused silica optical fibers," *J. Chem. Phys*. vol. 76(4), pp. 1712–1722, 1982.

[14] K. M, Davis and M. Tomozawa, "Water diffusion into silica glass: structural changes in silica glass and their effect on water solubility and diffusivity" *J. Non-Crystalline solids vol.* 185(3), 203-220, 1995.